Indian Journal of Pure & Applied Physics
Vol. 53, March 2015, pp. 199-211

New magnetic measurement system for determining metal covered mines by detecting magnetic anomaly using a sensor network

Yavuz Ege[a]*, Adnan Kakilli[b], Hakan Çıtak[c], Osman Kalender[d], Sedat Nazlıbilek[e] & Mehmet Gökhan Sensoy[f]

[a]Balikesir University, Necatibey Faculty of Education, Department of Physics, 10100, Balikesir

[b]Marmara University, Technical Education Faculty, Electrical Education Department, 34730, İstanbul, Turkey

[c]Balikesir University, Balikesir Vocational High School, 10100, Balikesir, Turkey

[d]Bursa Orhangazi Universtiy, Department of Electrical-Electronics Engineering, 16350, Bursa, Turkey

[e]Atilim University, Faculty of Engineering, Department of Mechatronics Engineering, 06830, Ankara, Turkey

[f]Middle East Technical University, Faculty of Arts and Sciences, Department of Physics, 06800 Ankara, Turkey

*E-mail: [a]Turkey,yavuzege@gmail.com, [b]kakilli@marmara.edu.tr, [c]hcitak@balikesir.edu.tr, [d]snazlibilek@atilim.edu.tr, [f]mehmetgokhansensoy@gmail.com

Received 27 February 2014; revised 9 July 2014; accepted 3 December 2014

The most commonly used remote sensing methods are used in such applications as the aquistic emmission, ground penetration radar (GPR) detection, electromagnetic induction spectroscopy, infrared imaging, thermal neutron activation, nuclear quadruple resonance, X-ray back scattering, neutron back scattering and magnetic anomaly detection. In deciding which type of method has to be used for detection, the variables such as the type of object, material used, position, geographical and environmental conditions, etc. play important roles. In recent years, studies are mainly concentrated on the improvement of detection distance, accuracy, power consumption aspects of remote sensing methods. In the present study, the same concerns are taken into account and a new magnetic measurement system is developed in this context. The system is made up of a sensor network consisting of high sensitive and low power anisotropic magneto-resistive KMZ51 sensors. The sensor network can detect the magnetic anomalies of vertical component of earth's magnetic field created by buried objects as metal covered mines. In the present paper, the effects of physical properties of metal covered materials to magnetic anomalies have been studied. The sensor network is composed of 24 sensors. The voltage levels of each sensor are measured one-by one and transferred to a digital computer where the distribution of the voltages in x-y plane is plotted as 3D graphics. Furthermore, the performance of the system on the detection of buried metallic mines and determination of their shapes have been investigated.

Keywords: Magnetic anomaly detection, Anizotropik magnetoresistive sensor, Metal covered mine, Magnetic measurement system

1 Introduction

Among the remote sensing methods, the applications such as the acoustics emission, ground penetration radar (GPR) detection, electromagnetic induction spectroscopy, infrared imaging, thermal neutron activation, nuclear quadruple resonance, X-ray back scattering, neutron back scattering and magnetic anomaly detection are the most commonly used. Although these systems are mainly used in health, traffic and military areas, they are also used in areas such as geology, archeology and civil engineering. In deciding which method has to be used, the type of object, material from which it is made, position of it, geographical and environmental conditions, etc play important roles. Principles of the commonly used methods may be given as in the following. The acoustic method depends on the sound waves with a frequency of below 1 kHz sent to ground and then collected by acoustic sensors[1,2]. The ground penetration radar (GPR) detection is based on the reflection of radio waves in the frequency range 1-1000 MHz from an object buried under ground[3,4]. The electromagnetic induction spectroscopy uses the signature over a wideband range of a secondary magnetic field when an object is subjected to a low frequency electromagnetic field[5,6]. The infrared (IR) imaging is a technique based on the detection of temperature differences of materials[7,8]. The neutron quadruple resonance method detects the nitrogen isotope (^{14}N) which is found in the composition of explosives. It is a radio frequency technique resembling the magnetic resonance (MR) technique[9]. Thermal Neutron Activation (TNA) is based on detection of gamma rays released by the activation of

nitrogen proton by electron bombardmant[10]. The neutron backscattering is another nitrogen activation process [11]. The X-ray backscatter uses accelerated photons that are passed through an object and the image on a photosensitive film[12] is obtained. The magnetic anomaly method of detection (MAD) is based on the determination of the amount of magnetic anomalies created by magnetic materials found in the environment[13-15]. In recent years, studies are mainly concentrated on the improvement of detection distance, accuracy, power consumption aspects of remote sensing methods. In magnetic anomaly detection (MAD) method, the accuracy of detection and identification of an object are directly proportional to the sensitivity of the sensor. Minimization of power consumption can be achieved by using actual earth magnetic field instead of creating an extra field creation.In most of the magnetic anomaly related studies made until now (except vehicle identification and traffic observations), an external magnetic field has been used[16-20]. The systems created under the works such as magnetic anomaly guidance system[21], magnetic anomaly sensing system[22], digital magnetometry[23] also use external magnetic fields. The present work has the capabilities of low power consumption and improved measurement accuracy. The reason for low power consumption is to use only sensors rather than using external sources for creating magnetic field. The systems found in the literature, use a lot of equipment that can result in high power consumption. Table 1 summarizes the equipment and power consumptions for different methods.

Furthermore, it is a new approach to sense the vertical component of earth's magnetic field and to identify the magnetic material based on it. The system developed here is used to analyse the effects of physical properties of metal covered materials to magnetic anomalies. The sensor network is composed of 24 sensors. The voltage levels of each sensor are measured one-by one and transferred to a digital computer where the distribution of the voltages in x-y plane is plotted as a 3D graphics. Furthermore, the performance of the system on the detection of buried metallic mines and determination of their shapes have been investigated. The sensor network uses sensors which are low power consuming and high accurate devices called KMZ51 anisotropic magnetoresistive elements.

A new magnetic field measurement system is developed here. By using the sensor network, all kinds of buried metallic materials such as metal covered mines can be detected by sensing the magnetic anomalies on vertical component of earth's magnetic field. The bridge accuracy of each sensor is determined by Eq. (1):

$$\text{Bridge accuracy}=\frac{\dfrac{\text{Bridge output voltage (mV)}}{\text{Bridge supply voltage (V)}}}{\text{Magnetic flux density of environment (G)}} \quad \ldots(1)$$

In the present work, the bridge supply voltage is 5 V, earths' horizontal magnetic flux density at our region is 0.5 G. With these values, bridge accuracy is determined as 0.635 (mV/V)/G. That is, every 1 Gauss change in magnetic flux density gives rise to a change of 0.635 mV in sensors' bridge output voltage. However, because of the magnetic anomaly in the region where the magnetic material is found, a small amount of earths' 0.5 G horizontal magnetic flux density may tend to vertical direction. In this case, the output voltage of the sensor bridge will give variations that are less than 0.635 mV. In order to get suitable readings, the output voltage of the sensor bridge is amplified by a gain of 1000, hence magnetic flux variations of 1 mG can be amplified to give a voltage of 0.635 mV. Furthermore, the readings of

Table 1 — Equipment and power consumptions of different methods of mine detection

Method	Equipment other than the sensor	Power consumed
Acoustic-seismic	Speaker, Laser Doppler Vibration meter	60 W
GPR	Rx and Tx antennas	10 W
EMI	Magnetic field source	190 W
IR	IR camera, Laser beam source	300 W
NQR	*RF* wave exciter	1000-2000 W
TNA	Electron accelerator	1000 W
Neutron back scattering	Neutron generator	1000 W
X ray back scattering	X ray source	1000 W

voltages are digitized with a resolution of 24-bit. This resolution gives a capability of transferring 149 nV variations to the computer environment. As a result, measurement system is improved[24,25] to sense magnetic flux densities of 2.34 μG.

2 Magnetic Measurement System

2.1 KMZ51 Anizotropik Magnetoresistive Sensor (AMR)

Today, a variety of sensors for measuring magnetic fiels is produced. Among them, the most popular and frequently used in experimental and industrial applications can be listed as follows:

- Induction coils, Hall sensors, Magnetoresistive sensors (AMR, GMR, CMR, TMR)
- Fluxgate sensors, Magneto-electric sensors, SQUID sensors.

The operation frequency ranges and the minimum and maximum detection limit values for magnetic fields of the above mentioned sensors are given in Table 2. Field values that the sensors (except the magnetoresistive sensors) can detect change directly proportional to applied frequency. On the other hand, magnetoresistivity is a change in electrical resistance under a magnetic field. Frequency dependence is mostly in question in induction coils[26].

While selecting an appropriate sensor type, primary and secondary parameters have to be taken into account. The primary parameters may be listed as range, bandwidth, accuracy, resolution, linearity, output signal behaviour, etc. The secondary parameters may be some physical, operational and economical properties such as operating temperature, sensors' geometry, chemical sensitivity, impedance, reliability, power consumption and cost[26,27]. Hence, a magnetoresistive sensor called KMZ51AMR is selected for this work because of its high sensitivity, low power consumption, operation in room temperature and low cost[28-30]. The sensors are arranged in groups of four as seen in Fig. 1. Each group is connected to the electronic control unit separately. The connection diagram is shown in Fig. 1.

2.2 D Scanning System

In the present work, a 2D scanning system moving within an area of 90×90 cm^2 has been developed. It is a position controlled system. It moves the sensor network platform over the ground both in x and y directions. It is made from wooden and aluminium plates and frames that do not have magnetic charactersitics.

Table 2 — Some typical values for magnetic field sensors[26]

Sensor Type	min. *B*	max. *B*	Operation frequency range
Induction coil	100 fT	Unlimited	0.1 mHz-1MHz
Hall sensor	10 nT	20T	0-100 MHz
Magnetoresistive sensor	100 pT	100mT	0-100 MHz
Fluxgate sensor	10 pT	1mT	0-100 MHz
Magneto-electric sensor	1 pT	-	0.1 mHz-1kHz
SQUID sensors	5 fT	1μT	0-100 kHz

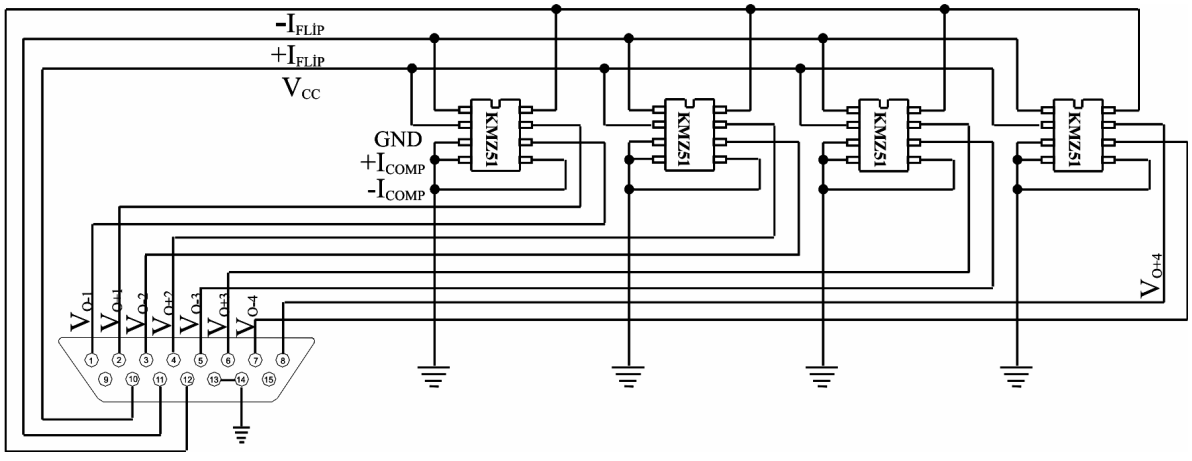

Fig. 1 — Connection diagram of a group of sensor network to electronic control unit

2.3 Soil Tank

A soil tank having the dimensions of 90x90x30 cm which are the length, the width and the depth of the tank respectively, is manufactured. Metal covered mines can be buried inside the tank for tests and experimentation purpose.

2.4 Electronic Control Unit

passed in a sequential order to a PC by a PIC 16F877A microcontroller (Fig. 2). The voltages $V_a=V_{o+}$ and $V_b=V_{o-}$ are first passed through optical isolators and then combined by means of a summing amplifier and inverted as a single output voltage. Next, the output voltage, $+V_{out}$=+AIN, is amplified by an AD524 amplifier which is adjusted by a knob mounted on the front panel of the electronic control unit. Depending on the applications needs, the voltage, $+V_{out}$, can be amplified by the gains of 100, 150, 200, 300, 500 or 900.

Amplified sensor voltage is converted to a digital value by means of 24-bit ADC, AD7714, and received by a PC through a parallel port. It is then stored in a text file created by the user. The ADC circuit developed here is shown in Fig. 3. A Visual Basic (VB) based program is developed for this purpose. The program can collect the data from all of the sensor blocks of the sensor network in sequence. A user can start the data collection by pressing a button mounted in front of the panel of the unit (Fig. 4).

Electronic control unit of the magnetic measurement system developed here is shown in Fig. 4.

2.5 Control Software for Magnetic Measurement System

The interface of the VB based data receiving software that is developed for the magnetic measurement system is shown in Fig. 5.

The developed software can provide the user the following information: (1) Record sheet during measurement; (2) Dimensions of the scanned area; (3) Position of the center of the sensors within the scanning area; (4) Movement directions of sensors

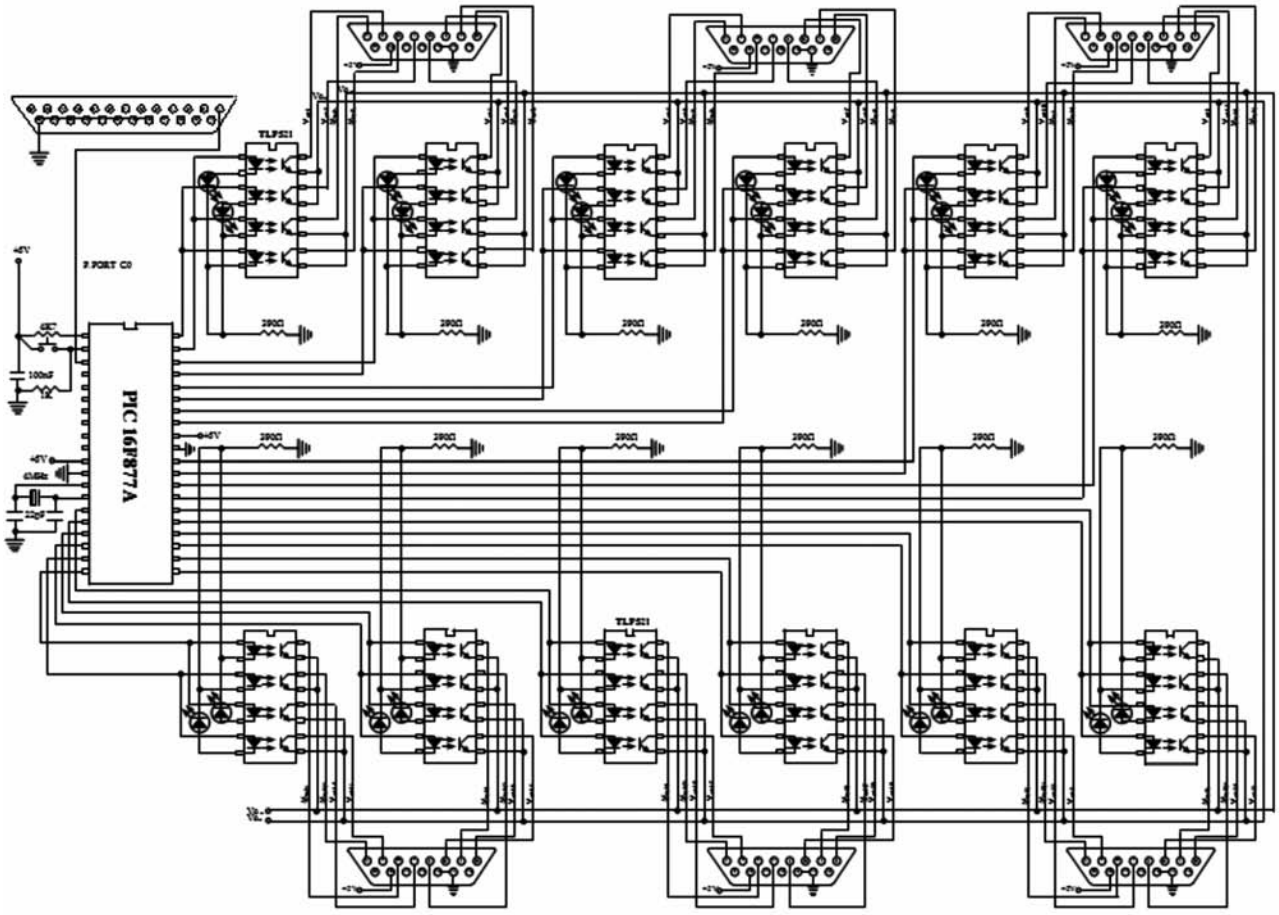

Fig. 2 — Sensor control circuit

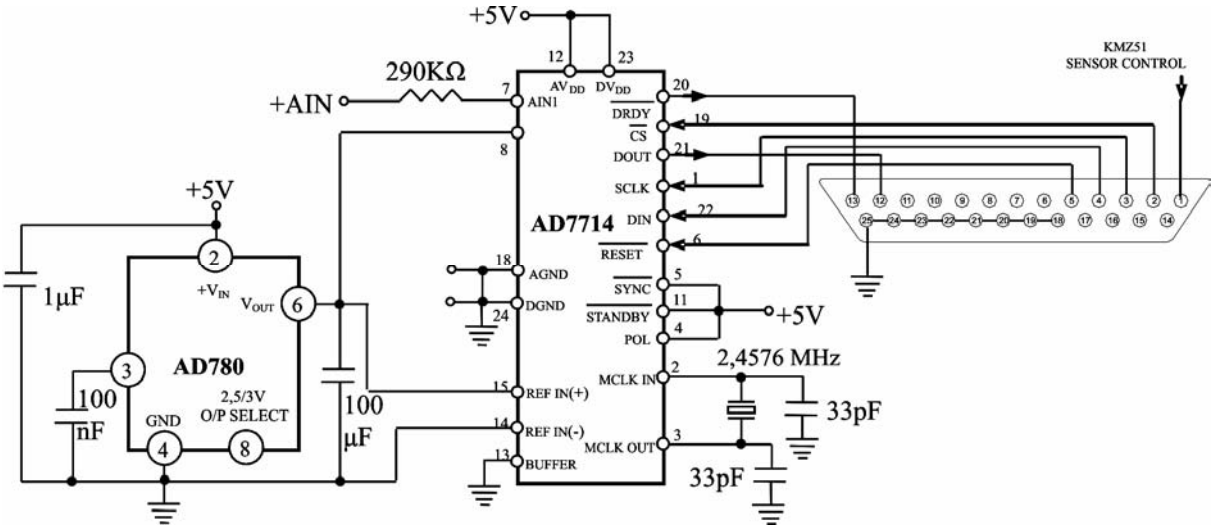

Fig. 3 — 24-bit analog to digital converter circuit

Fig. 4 — Electronic control unit of the magnetic measurement system developed here

within the scanning area; (5)Values of sensor voltages at the target points reached; (6)2D graphics of the instantaneous sensor voltages at X position; (7) All records of variables related to the measurements when the tests are breaked for any reason; (8) 3-D graphics of voltage variations at the end of the scaning process.

The developed software programme is activated by the "Start" button. If the Start button is not pushed, then the port is checked in every 1 s. Fig. 6 shows the 2D graphical interface. 3D graphical interface is shown in Fig. 7. An example of mine detection work is shown in Fig. 8. The photograph of the testbed developed in this work is seen in Fig. 9.

3 Experimental Set-up

Experimental work is carried out by using actual mines. In our study, first of all an M2 type anti-personnel land mine with a diameter of 5.6 cm and a

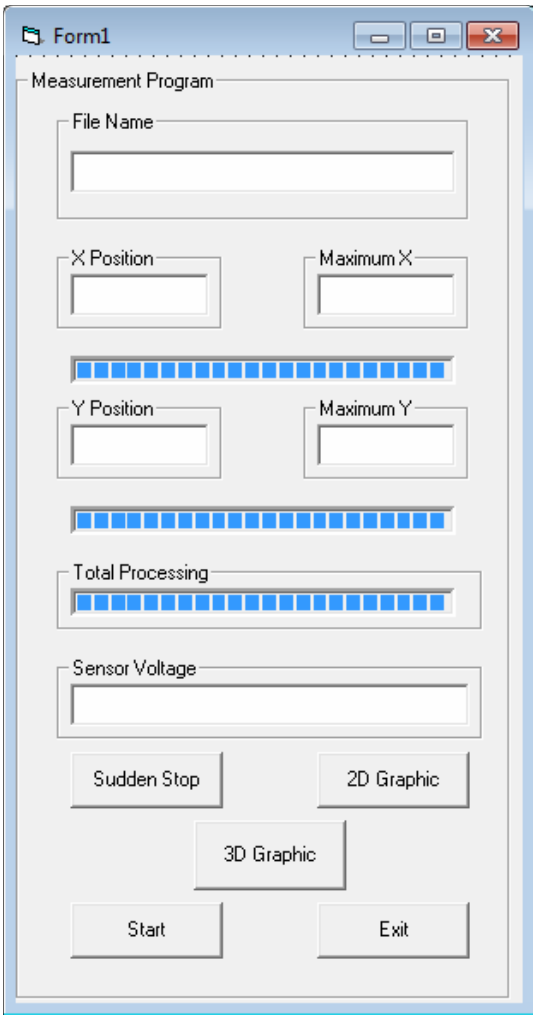

Fig. 5 — Interface of the VB based data receiving software that is developed for the magnetic measurement system

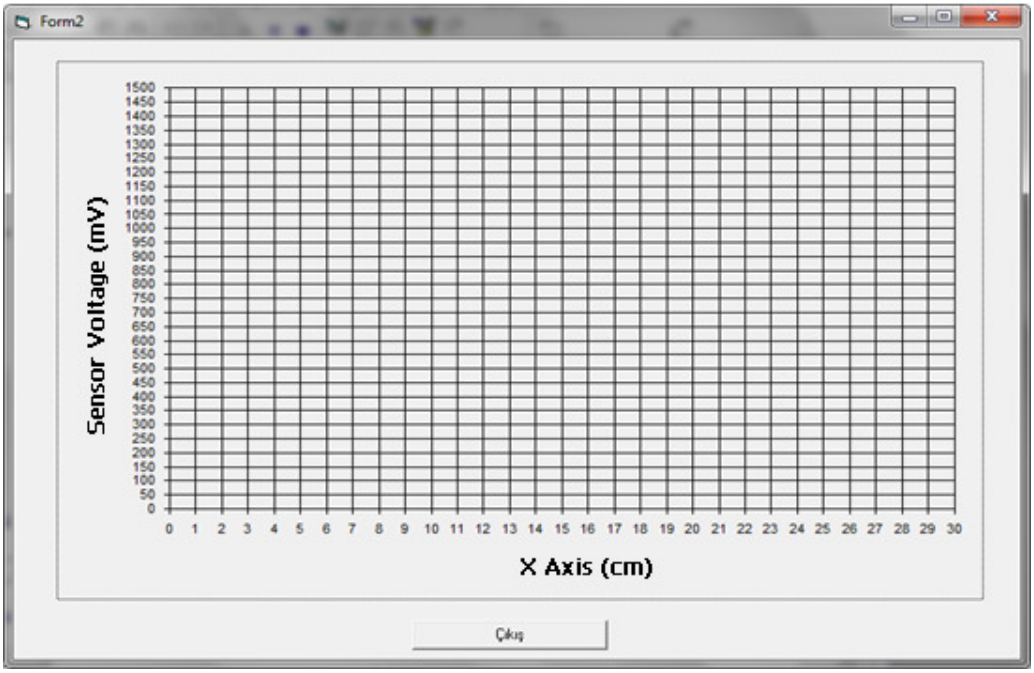

Fig. 6 — 2D Graphical interface

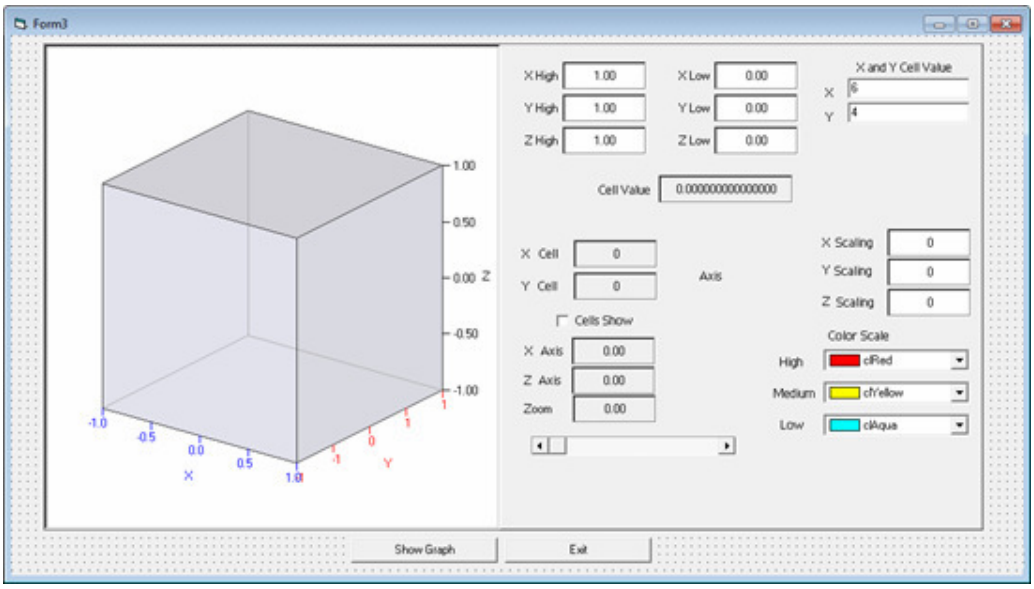

Fig. 7 — 3D Graphical interface

height of 16 cm is placed to the scanning region of our measurement system. The sensor network platform is then approached to a height of 9 cm above the mine and moved with a step size of 4.8 cm. At each step, the sensor output voltages are measured. But, it is not possible to determine its diameter at all heights. The diameter of the land mine can be determined experimentally when the scanning distance between the sensor plate and the top of the mine is about 5 cm. The effect of the distance between the sensor plate and the mine and the sensor output voltage versus scanning height has been investigated is plotted in Fig. 10.

Figure 10 shows that at the most 0.7 V voltage can be obtained from a AMR sensor network which is at a height of 22 cm above the M2 anti-personal mine. This

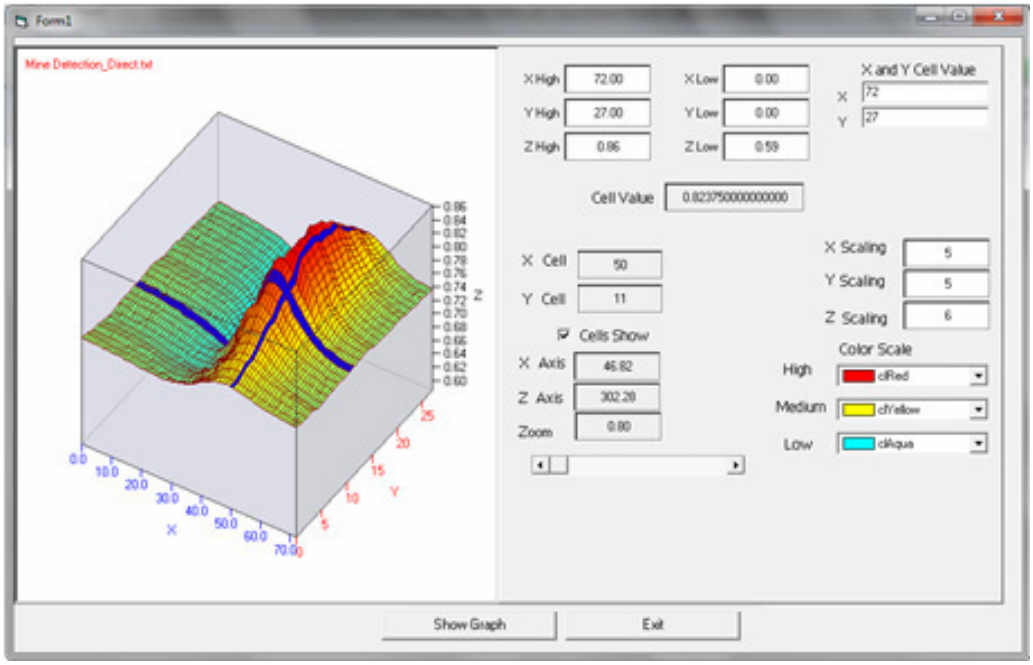

Fig. 8 — An example of 3D graphics of magnetic anomaly by a land mine

Fig. 9 — Test bed of the magnetic measurement system

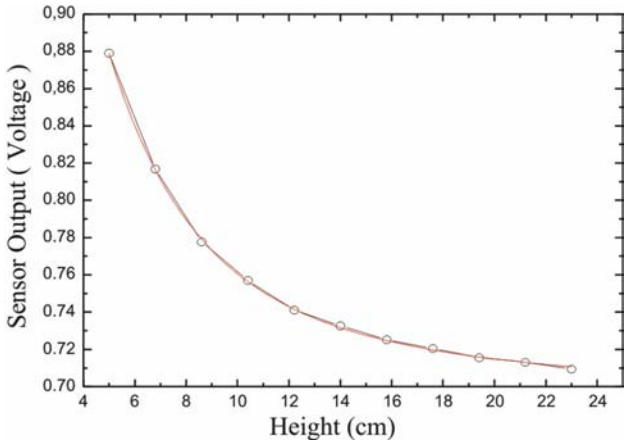

Fig. 10—Sensor output voltage vesus scanning height for M2 type anti-personnel mine

measured value is considered as the reference when no mine is available on the environment. For this reason, it is not possible to detect M2 mines above 22 cm by using our system. However, if an external magnetic field is used instead of earth's magnetic field, then the maximum detection height may change. Also, a mine having more metal content than an M2 mine can be detected from a higher distance than 22 cm. That is, the magnitude of magnetic anomaly and the magnitude of the voltage from the sensor network will depend on the metal content of the mine and the value of earth's magnetic field over the environment. But, under this limit, there is no difficulty to determine a metal covered mine.As seen in Fig. 5, it can be understood that an AMR sensor network with a height of 22 cm above the mine cannot detect the existance of a M2 type anti-personnel mine. In our study, secondly, we placed a M16 type anti-personnel mine with a diameter of 11 cm and a height of 12 cm under the scanning platform and the sensor voltages are read when the distance between the sensor plate and the mine is 9 cm. The voltages were read again with a step size of 4.8 cm. The magnetic measurement system can detect

the existence of the land mine. But, it is not possible to determine its diameter at all heights. The diameter of the land mine can be determined experimentally when the scanning distance between the sensor plate and the top of the mine is about 5 cm. In the present study, the effect of the distance between the sensor plate and the mine has been investigated and the voltage values for each steps of heights are recorded. The values versus distances are plotted as seen in Fig. 11.

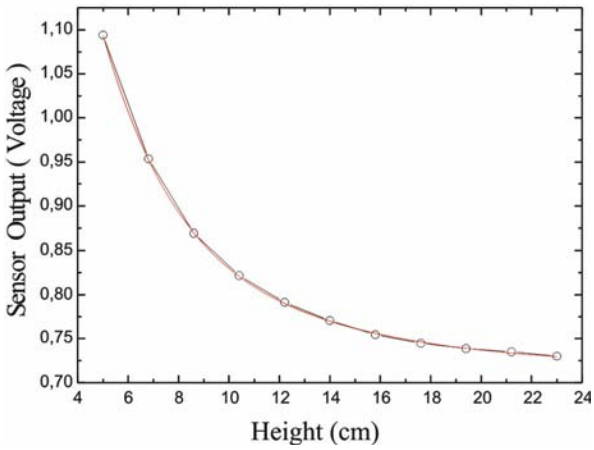

Fig. 11—Sensor output voltage versus scanning height for M16 type anti-personnel mine

4 Performance of Magnetic Measurement System on Mine Determination

A magnetic measurement system is developed and it is composed of a mechanical system providing a three dimensional movement of a sensor network platform that is used for sensing the variation of earth's magnetic field, an electronic control system that can process the data coming from the sensors and send them to a computer and a software can evaluate and record the data.In the present research study, we separately considered variables such as tick of material, the angle between horizontal plane, width of material, number of objects within the environment, etc. and the changes in the output voltages of the sensors due to magnetic anomaly have been measured and the gray-scale graphics have been plotted. As a result, by means of the magnetic measurement system, the followings have been determined experimentally:

Top view of a sample can be determined by scanning the area. It depends on the detection distance of the sensor network and the angle between the platform and the sample. Shape of the sample (either prismatic or cylindrical) facing the sensor network platform can be determined.

In Fig. 12, the coloured graphics of the sensor network output voltages over the scanned area for the

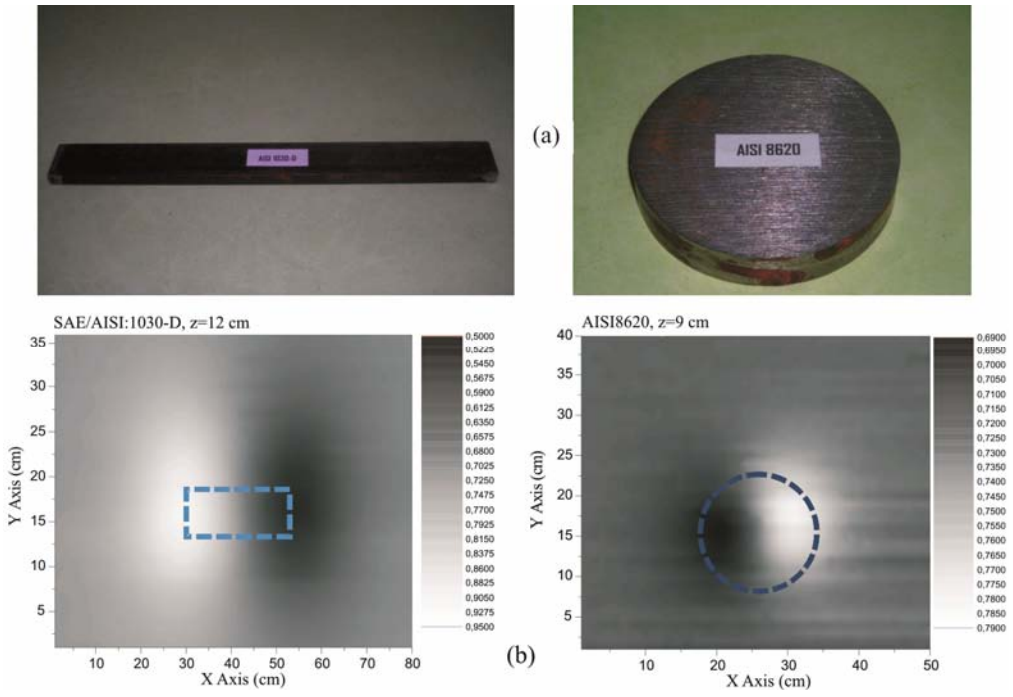

Fig.12-AISI1030-D and AISI8620 samples, (a) their photographs (b) coloured images of the sensor output voltages with respect to scanning area

samples of AISI1030-D ve AISI8620 are given. Noting the images that show the faces looking at the scanning side, it may be understood that the first one at the left-hand side is a prismatic and the other is cylindrical sample.

In the present study, a sample of AISI1030-C with a length of 10 cm, a width of 3 cm and a thickness of 0,5 cm is used. By keeping the other properties fixed, the thickness of it is changed gradually starting from 1 cm to 5 cm with the steps of 0.5 cm. It is repeated for 9 samples. The samples are scanned through the x-axis. The sensor is moved just over the sample (along the sample) with discrete steps of 1 cm and the sensor output voltage is read at each step. The readings are plotted as shown in Fig. 13. As seen from the graph, the level of each characteristic curve is increased as the thickness is increased. The maximum values of the sensor's output voltages are determined from the graphs for each curve and "thickness versus sensor's output voltage" relation is shown in Fig. 14. The output voltage of the sensor increases directly proportional to the thickness of the material. The sensor used in the measurement system can have an accuracy of detecting the thickness variations of 0.5 cm. If the sample under consideration has known properties other than the thickness and if a characteristics curve similar to the one shown in Fig. 14, is available in the database, then the thickness of the sample can easily be determined from the maximum output value of the sensor.

It is determined that the magnetic anomalies created by the samples with the same properties but making different angles with the horizontal plane are different from each other. By using this information, the angle with horizontal plane can be determined.

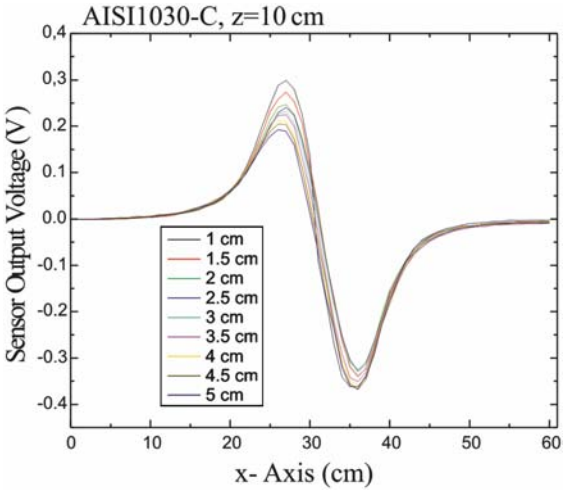

Fig. 13 — Single axis scanning of AISI1030-C sample with different thicknesses

In order to give an example for the determination of the angle that a prismatic sample makes with the plane, a couple of graphics obtained by a single-axis scanning process from a AISI1030-C sample making different angles with the horizontal axis are shown in Fig. 15. There is no noticeable change in the minimum pick values of the output signal as the angle between the sample and the horizontal axis increases. However, the signal level at maximum pick has decreased because of the reason that the sample away from the sensor with the angle between the sample and the horizontal axis is increased.

In the present case as shown in Fig. 16 the magnitude of sensor's minimum voltage can be obtained for a different distance of x that the displacement, y, of the center of the sample making an angle of α may be written as in Eq. (2):

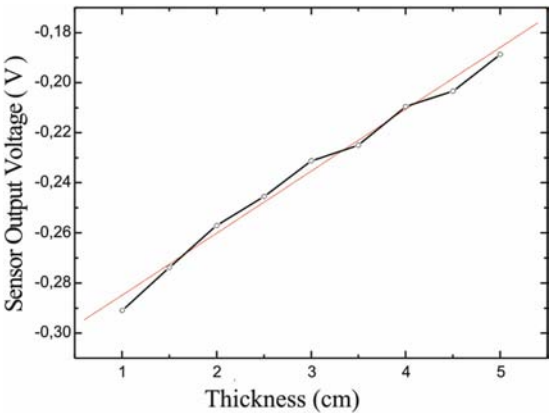

Fig. 14 — Thickness versus sensor's output voltage for AISI1030-C sample

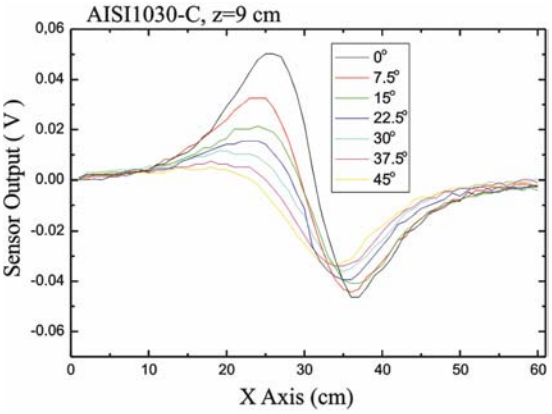

Fig. 15—Form of signals of sensor output voltage with respect to x axis during the single-axis scanning process using AISI1030-C sample. The place of the center of the sample changes as the angle increases

$$y = 2r\sin^2(\alpha/2) \quad ...(2)$$

In Fig. 17, the scanning results are given for a AISI1030-C sample making angles of both 0° and 30° with the plane from a height of z=9 cm for each case. Fig. 17(a and b) shows that the black-and-white ellipses are equal when the angle between the sample and the plane is 0^o. But, when the angle is 30°, the dark ellipse becomes dominant than the light ellipse. The reason for it is that the one end of the sample making the angle with the plane is close to the sensor.

The maximum sensor output voltage (Fig. 15) versus displacement of center of the sample is shown in Fig. 18. As seen in Fig. 18, the best sensor output voltage can be obtained while the angle between the sample and the plane is 0^o. The output voltage decreases with the increase of angle. If all of the properties except for the angle with the plane is known and if the curve in Fig. 18 is available, then the angle can be determined from thr maximum values of the sensor output voltages. The maximum sensor output voltage gives the deviation of the center of the sample and from which the angle with the horizontal axis can be obtained using Eq. (2).

Dimensions such as diameter and length of a sample can be determined by means of sensor voltage characteristics for each specified sample.

As it may be understood from the coloured graphics of the sensor network, output voltages belonging to two samples in Fig. 19(a), the length of the prismatic sample is about 25 cm and the diameter of the cylindirical sample is about 15 cm. Actual dimensions are as follows: the prismatic sample has a length of 28 cm, while the cylindirical sample has a diameter of 14 cm.

In some limited conditions, top view images of several samples can be found.Samples with the same or different geometry can be separated by detecting the sections facing the sensor network platform.

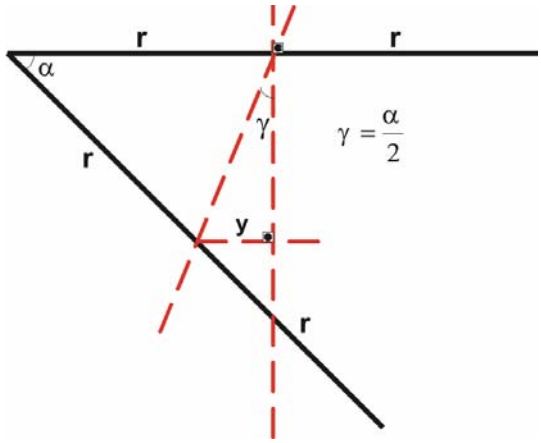

Fig. 16—Change in the place of the center with the angle between the sample and the horizontal plane

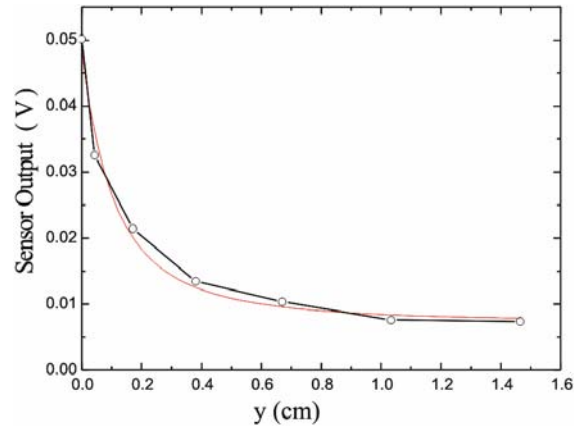

Fig. 18—Deviation of center versus sensor output voltage for AISI1030-C

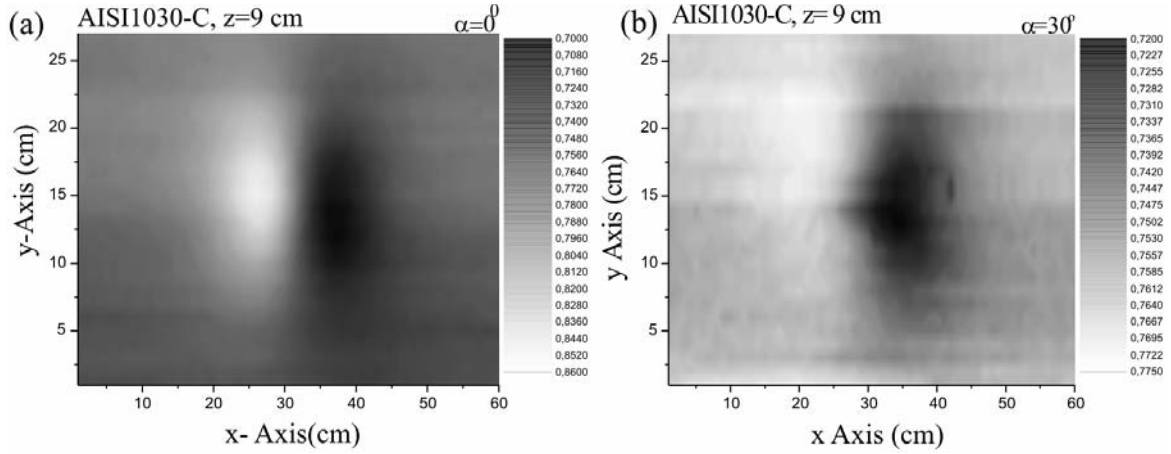

Fig. 17—Results of x-y area scanning for AISI1030-C sample making an angle of.(a) 0°; (b) 30°

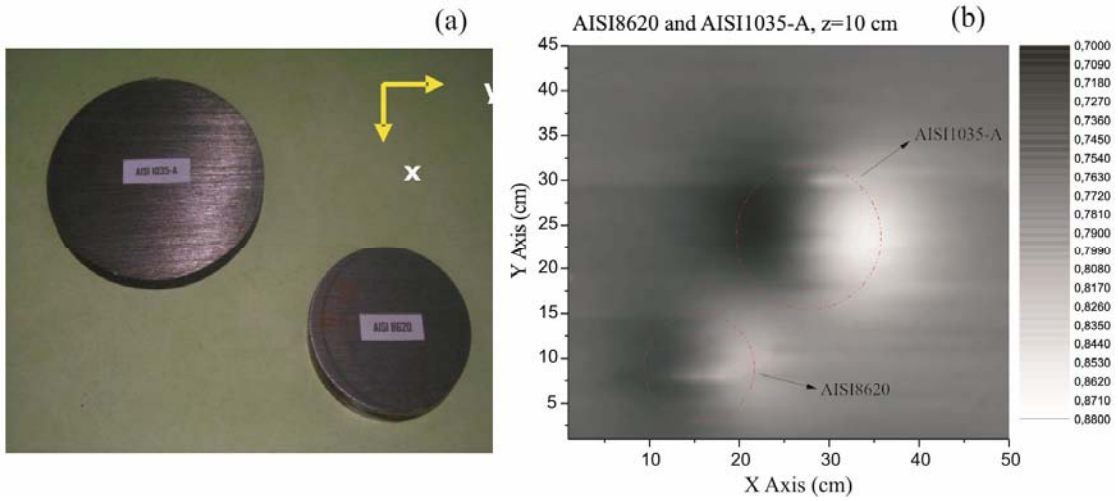

Fig. 19—AISI8620 ile AISI1035-A samples, b) the sensor network output voltage image at the x-y plane of x-y

In the present work, as a third case, two cylindrical samples are located at a distance of 4 cm between them in the scanning area as shown in Fig. 19(a). The output of the sensor network at x-y plane when z=10 cm is shown in Fig. 19(b).

It is noted that there are two samples at the scanning area and both of them are cylindrical in shape. In addition, the voltage variations of the sensor network related to two samples can be distinguished from each other. Therefore, the boundary for separating the two samples may be said that it is about 3-4 cm for the magnetic measurement system. When they come closer than this limit, the images may occlude each other.

The magnetic measurement system developed here can easily be used in military applications. Measurement characteristics can be used to distinguish whether the object is a mine or a can.

For this reason, an M16 anti-tank mine together with a can having the same dimensions as the anti-tank mine at the same scanning area has been located. When the height of the sensor network and the mine is about 9 cm, the output voltage variations of the sensor network elements through the x-y plane are determined with a step distance of 1 cm.

The magnetic measurement system that is developed, has some advantages on the similar systems found in literature. We can list these advantages as follows:

It utilises earth's magnetic field instead of an external magnetic source. This reduces the energy consumption of the system. The magnetoresistive sensor has a high sensitivity as compared to other types of similar sensors.The output of the electronic control unit can easily be adjusted to a desired level before starting the experiment.Micro level voltage variations can be transferred to the computer by a 24-bit ADC.The magnetic measurement system cannot be affected by the external magnetic disturbances and noises.

Our measurement system can work based on the voltage values taken by the sensor network before hand. The maximum voltages that can be measured from different kinds of mines and samples are stored in the database. When the level of voltages higher than the levels stored in the database is obtained in an application, it can be concluded that the object found in the environment may be a permanent magnet. The levels stored in the database can be some probabilistic parameters such as mean value or standard deviation. Therefore, in order to draw a correct reasoning, the volume of the database must be large enough. The developed system is a user friendly and very cost effective system.

There are some other techniques and systems widely used in applications. Among them, we can give the examples such as acoustic-sismic, ground penetration radar (GPR) and electromagnetic induction (EMI) for the determination of mine cover. These types of equipments are very expensive. The prices[32-34] may vary from 10 000$ to 30 000 $. However, the system that we developed may cost about 2 000 $ (Table 3). The geographical locations[35] have been taken into account since the detection of mines largely depends on the geographical and environmental conditions. In that study, a GPR

Table 3 — Other methods of mine detectionand unit prices

Method	Equipments	Unit Price	Purpose
Acoustical seismic	Laser-Doppler VibrationTransdusers	21 000$	Mine cover (Plastic+Metal)
Ground Penetration Radar	GPR system, transmitter antennas	25 000$	Mine cover (Plastic+Metal)
Electromagnetic Induction	Induction coil, Magnetometer,Conduction meter	10 000$	Mine cover (Metal)
Infrared İmaging	Thermal Camera	15 000$	Mine cover (Plastic+Metal)
Neutral Quadruple Resonance	*RF* exciter, detector	14 000$	Mine explosive
Thermal Neutron Activation	Electron accelerator, Gamma detector	20 000$	Mine explosive
Neutron Backscattering	Electron accelerator, Electron detector	23 000$	Mine explosive
X-Ray Backscattering	X ray source,Backscattering detector	14 000$	Mine explosive
Magnetic Anomaly (Other Applications)	External Magneticfield source, Magnetic detectors, Mechanical system	10 000$	Mine cover (Metal)
Magnetic Anomaly (Our system)	Sensors, Mechanical system	2000$	Mine cover (Metal)

mounted on a vehicle at three different geographical locations is used. The data used in the test were acquired from over 6000 m^2 of simulated dirt and gravel roads and also off-road conditions. These data contained approximately 300 landmine signatures, over half of which were plastic-cased or completely non-metal.

Maximum detection heights are specific to the region of earth and they may change depending on the country where experiments are carried out. If an external magnetic field is used instead of earth magnetic field, then the maximum detection distance may increase.

5 Conclusions

The M2 and M16 anti-personnel mines are metal covered mines and these types of mines can easily be determined by the magnetic measuement system developed here. However, there are some military mines that have plastic covers. Only the detent pin is a metallic material in these types of mines. This pin may create a small amount of magnetic anomaly and the voltage of the sensor becomes very little. The gain of the amplifier should be at least 900 in order to detect such a mine.The developed magnetic measurement system has a measurement capability of buried magnetic objects up to the depth of about 22 cm. This is not the capability of the measurement system, but the effect of objects on the earths' magnetic field. That is, if a buried object creates a magnetic anomaly that is deeper than any other object, then the measurement system can measure it from a height of much greater than 22 cm. It depends on the magnetic permeability and the density of the magnetic material.

In some important studies, geographical locations have been taken into account since the detection of mines largely depends on the geographical and environmental conditions. For example, in a study, a GPR mounted on a vehicle at three different geographical locations is used. The data used in the test were acquired from over 6000 m^2 of simulated dirt and gravel roads, and also off-road conditions. These data contained approximately 300 landmine signatures, over half of which were plastic-cased or completely non-metal. As a matter of fact, geographical and environmental conditions affect the results largely. In our approach, the magnetic anomalies of the earth over the regions have been utilized. This method somehow facilitates data collection in different locations with different conditions. The sensor network used in our system eliminates some faulty alarms since we concentrate on highly metallic land mines.

References

1 Simeone F, *Nucl Instruments & Methods In Phys Res*, 604 (2009) 196.
2 Habib Maki K, *Sensor Lett,* 5 (2007) 500.
3 Frigui H & Gader P, *IEEE Trans On Fuzzy Sys*, 17 (2009) 185.
4 Belli K, Zhan H & Wadia-Fascetti S, *IEEE Trans On Geosci & Remote Sensing*, 47 (2009) 3656.
5 Soleimani M, *IEEE Trans on Instrumentation & Measurement*, 59 (2010) 553.
6 Robledo L, Carrasco M & Mery D, *Int J Remote Sensing,* 30 (2009) 2399.
7 Brett D J L, Aguiar P, Clague R, Marquis A J, Schöttl S, Simpson R & Brandon N P, *J Power Sources*, 166 (2007) 112.
8 Meola C, *Materials Lett*, 61 (2007) 747.
9 Gregorovic A & Apih T*, J Magnetic Resonance*, 198 (2009) 215.

10 McFee John E, Faust Anthony A, Andrews H Robert, Kovaltchouk V, Clifford Edward T & Ing H, *IEEE Trans on Nucl Sci*, 56 (2009) 1584.

11 Haušild P, Davydov V, Drahokoupil J, Landa M & Pilvin P, *Materials & Design,* 31 (2010) 1821.

12 Faust A A, Rothschild R E, Leblanc P & McFee J E, *IEEE Trans on Nucl Sci*, 56 (2009) 299.

13 Ege Y, Sensoy M G, Kalender O, *IEEE Trans On Instrumentation & Measurement*, 60 (2011) 3140.

14 Ege Y, *Sens Actuators-A Physic*, 147 (2008) 52.

15 Kang M H, Choi B W & Koh K C, *Sens & Actuators A-Physic*, 118 (2005) 278.

16 Woloszyn M, *Polish Maritime Res*, 15 (2008) 77.

17 Galanzha E, Shashkov E V, Kelly T, *Nature Nanotechnology*, 4 (2009) 855.

18 Piro S, Samir A & Versino L, *Annali Di Geofisica*, 41 (1998) 343.

19 Vyhnanek J, Janosek M & Ripka P, *Sens Actuators-A Physic*, 186 (2012) 100.

20 Ripka P, Lewis A M & Kubik J, *Sensor Lett*, 5 (2007) 15.

21 Braithwaite Jason J, *J Parapsychology*, 69 (2005) 151.

22 Kushwah V, Singh V & Singh B, Phys & *Chem of the Earth*, 32 (2009) 367.

23 Riggs L S, Mooney J E & Lawrence D E, *IEEE Trans on Geosci & Remote Sensing*, 39 (2001) 56.

24 Nazlibilek S, Ege Y & Kalender O, *Measurement*, 42 (2009) 1402.

25 S Nazlibilek, O Kalender & Y Ege, IEEE *Trans on Instrumentation & Measurement,* 60 (2011) 1028.

26 H Hauser, G Stangl, W Fallmann, R Chabicovsky & K Riedling, "Magnetoresistive Sensors", Institut für Industrielle Elektronik und Materialwissenschaften TU Wien, Preparation, Properties and Applications of Thin Ferromagnetic Films, June (2000).

27 Junyi Zhai, Zengping Xing, Shuxiang Dong, Jiefang Li & Viehland D, *Appl Phys Lett*, 88 (2006) 062510.

28 Kang M H, Choi B W, Koh K C, Lee J H & Park G T, *Sens Actuators-A Physic*, 118, (2005) 278.

29 Dimitropoulos K, Grammalidis N, Gragopoulos I, Gao H, Heuer Th, Weinmann M, Voit S, Huhnold M, Stockhammer C, Hartmann U & Pavlidou N, *Engineering & Teechnology*, 19 (2008) 815.

30 Kim H & Shoji T, *Adv In Nondestructive Evaluation,* 270 (2004) 625.

31 Baldoni J A & Yellen B B, *Trans on Magnetics*, 43 (2007) 2430.

32 Robledo L, Carrasco M & Mery D, *Int J Remote Sensing*, 30 (2009) 2399.

33 Belli K, Zhan H & Wadia-Fascetti S, *IEEE Trans on Geosci & Remote Sensing*, 47 (2009) 3656.

34 Ramachandran G, Gader P D & Wilson N*, IEEE Trans on Geosci & Remote Sensing,* 7 (2010) 535.

35 Gader P D, Mystkowski M & Yunxin Zhao, *IEEE Trans on Geosci & Remote Sensing,* 39 (2001) 1231.